

5-12-1985

Analysis of Minerals Using Specimen Isolated Secondary Ion Mass Spectrometry

J. B. Metson
University of Western Ontario

G. M. Bancroft
University of Western Ontario

H. W. Nesbitt
University of Western Ontario

Follow this and additional works at: <https://digitalcommons.usu.edu/electron>

 Part of the [Biology Commons](#)

Recommended Citation

Metson, J. B.; Bancroft, G. M.; and Nesbitt, H. W. (1985) "Analysis of Minerals Using Specimen Isolated Secondary Ion Mass Spectrometry," *Scanning Electron Microscopy*. Vol. 1985 : No. 2 , Article 11.
Available at: <https://digitalcommons.usu.edu/electron/vol1985/iss2/11>

This Article is brought to you for free and open access by the Western Dairy Center at DigitalCommons@USU. It has been accepted for inclusion in Scanning Electron Microscopy by an authorized administrator of DigitalCommons@USU. For more information, please contact digitalcommons@usu.edu.

ANALYSIS OF MINERALS USING SPECIMEN ISOLATED SECONDARY ION MASS SPECTROMETRY

J.B. Metson,[†] G.M. Bancroft,⁺ and H.W. Nesbitt^{*}

[†] Surface Science Western, ⁺ Department of Chemistry and ^{*} Department of Geology
University of Western Ontario, London, Ontario, Canada N6A 5B7

(Paper received January 19 1984, Completed manuscript received May 12 1985)

Abstract

Considerably improved suppression of molecular ions in secondary ion mass spectrometry (SIMS) spectra of nonconductor minerals has been obtained using a CAMECA IMS-3f ion microscope with unconventional operating conditions [so-called specimen isolated (SI) conditions]. In a zircon spectrum close to forty elements are positively identified and molecular ions such as oxides and hydrides have very low intensities. Thus, with a $^{28}\text{Si}^+$ intensity of 10^6 cps, the Si^+/SiO^+ ratio is 10^5 , and the $^{30}\text{SiH}^+$ intensity is low enough to enable quantitative analysis using $^{31}\text{P}^+$ down to 0.01 wt % P_2O_5 in a silicate glass matrix. The SI conditions enable us to follow major, minor and trace element concentrations across a complex alteration zone such as a sphene/hornblende contact. Isotope ratios show reasonable agreement with natural isotopic abundances, but relatively large "kinetic energy" induced isotopic fractionation is observed due to our analysis of high kinetic energy secondary ions. For zircon, and sphene samples, the isotope fractionation plotted against the mass ratios of the isotopes shows a linear dependence.

Introduction

The development of Secondary Ion Mass Spectrometry (SIMS) as a major tool in geochemical analysis has been foreseen for some time^{4,14}. However in practice, the development of SIMS has been slowed by considerable difficulties in quantifying secondary ion yields from complex matrices. Part of this difficulty arises from molecular ions which interfere with the detection of isobaric elemental ions. The second and more fundamental problem is the complex nature of the sputtering and ionization process which is strongly affected by both the sputtered matrix and the nature of the primary beam. A further major difficulty specific to non-conducting samples such as most minerals, is instability of the secondary ion signal due to uncontrolled charging of the specimen surface¹⁹.

This paper deals with several of the problems outlined above, but is primarily addressed to obtaining clean elemental ion peaks in the secondary ion spectrum. Interferences can be alleviated in the mass spectrometer by the use of either high mass resolution¹ or kinetic energy filtering of the secondary ions¹⁶. Both methods can result in effective resolution of many elemental ions from molecular species, but both have limitations in that they often sacrifice considerable intensity and thus can severely affect sensitivity. In the case of high mass resolution, $M/\Delta M$ up to 5000 causes only a small intensity loss typically an order of magnitude. Thus for example the resolution of $^{31}\text{P}^+$ from $^{30}\text{SiH}^+$ is not difficult. However the method is of very limited use for the rare earths as an $M/\Delta M$ in excess of 10,000 is necessary to separate the simplest molecular ions i.e., heavy rare earth peaks from light rare earth oxides, and the intensity loss is often prohibitive¹². Conventional energy filtering is again useful in specific applications and has provided the best approach so far to quantitative analysis. However a 125 eV voltage offset usually results in at least a two orders of magnitude drop in intensity. Furthermore even this degree of offset may not be sufficient. Again, to use the rare earths as an example, a 125 eV offset improves M^+/MO^+ to only ~ 20 .

KEY WORDS: Secondary Ion Mass Spectrometry, Mineral Analysis, Specimen Isolation, Molecular Ion Suppression, Isotopic Fractionation, Zircon.

Address for correspondence:

J.B. Metson
Surface Science Western
Natural Sciences Centre, University of Western
Ontario, London, Canada N6A 5B7

Phone no.: (519) 679-2233

The specimen isolation method^{2,5,8} has been shown to exploit an extreme form of kinetic energy filtering, utilizing the high energy tail of the secondary ion energy spectrum to suppress molecular ion interferences and stabilize surface charging. Metson et al⁸ demonstrated the application of the method to mineral specimens with element/oxide ratios better than 10^4 for $^{48}\text{Ti}^+ / ^{48}\text{TiO}^+$, 2×10^3 for $^{89}\text{Y}^+ / ^{89}\text{YO}^+$, and $5 \times 10^2 \rightarrow 1 \times 10^3$ for $^{164}\text{Dy}^+ / ^{164}\text{DyO}^+$ from sphene (CaTiSiO_5) samples. Peak intensities for Ca, Ti and Si under these conditions are still $\sim 10^6$ cps. Using this technique McIntyre et al⁶ showed elemental ion/oxide ratios better than 5×10^4 for $^{56}\text{Fe}^+ / ^{56}\text{FeO}^+$ and 1.7×10^5 for $^{52}\text{Cr}^+ / ^{52}\text{CrO}^+$ from stainless steel specimens, while from pure silicon $^{28}\text{Si}^+ / ^{28}\text{SiO}^+$ $\sim 1 \times 10^5$ was recorded under specimen isolation conditions. Using energy offset conditions to analyze ions of 125 ± 5 eV, these numbers were respectively 1×10^3 , 1×10^3 and $\sim 5 \times 10^2$.

S.I. conditions have now been demonstrated in a variety of mineral analysis applications including trace element and rare earth analysis of a number of accessory minerals^{7,8,9,10}. In this paper we discuss several additional applications of the specimen isolated method, such as phosphorous determinations in whole rock powers, determination of trace element partitioning at mineral interfaces and measurement of isotopic abundances.

Experimental

The results described below were obtained on a Cameca IMS 3f secondary ion microscope. The instrument is an electrostatic sector/magnetic sector instrument with a double focussing geometry, and is thus capable of both high mass resolution ($M/\Delta M \sim 10,000$) and energy selection of secondary ions. Kinetic energy selection is traditionally accomplished either by offsetting the secondary ion accelerating voltage applied to the sample, or by translation of an energy slit located between the electrostatic and magnetic sectors.¹⁶ The primary ion beam used was mass filtered $^{16}\text{O}^-$ at a net accelerating voltage of $14.5 \rightarrow 16$ kV. In our measurements, the entrance and exit slits, field aperture and contrast aperture of the secondary column are wide open, resulting in minimum mass resolution ($M/\Delta M \sim 250$) and a broad energy window (~ 130 eV)^{5,6,8}.

The extreme form of energy filtering in the SI mode is achieved through the use of a modified sample holder in which the sample (usually uncoated) is insulated from the secondary accelerating voltage, and exposed to the primary beam through a circular aperture of 3 mm diameter in the sample holder face (Figure 1). This hole size has been shown to give the best compromise between sensitivity and molecular ion suppression^{5,6}. The primary beam causes the sample to charge negatively, with respect to the sample holder and creates a potential difference of up to ~ 700 eV between the two². Steady state charging is attained within a few seconds and stable secondary ion signal (within $\pm 1\%$ over 15 minutes) results. The degree of charging can be partially controlled through varying the primary beam current, or more effectively by altering the aperture size of the sample holder². The

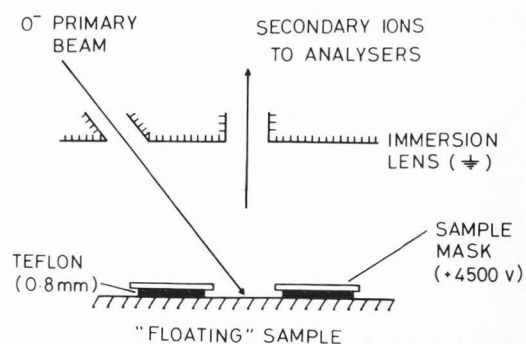


Figure 1. The specimen holder arrangement for specimen isolated SIMS. The dimension of the aperture in the sample mask (3 mm) is critical in achieving stable, reproducible charging.

requirements for sensitivity and stable reproducible charging, impose a minimum possible beam diameter of $40\text{--}50 \mu\text{m}$, and up to $100 \mu\text{m}$ when operating with maximum sensitivity. This is determined by the charge dissipating ability of the sample (i.e. smaller beams can be used on more conductive samples) and the spreading of the primary beam by the electric field above the beam impact zone. Thus true microanalysis would require either the use of the field aperture in the secondary column to restrict the analysis area, or some raster-gating of the secondary ion counting system. Preliminary investigations of ion images from a Cu/Al grid under SI conditions indicate that from a conducting sample insulated from the secondary accelerating voltage and charging ~ 450 eV, ion trajectories are not significantly distorted and thus the field aperture could be used to restrict the analysis area on such samples. However, either procedure would be accompanied by some loss of sensitivity and improved control of primary beam spot size would be preferable, perhaps with a variable aperture over the sample surface.

Results and Discussion

The application of energy filtering at the specimen surface with this method results in excellent transmission of high energy ions through the secondary column, particularly through the use of a broad energy window (~ 130 eV) and contrast aperture. Available intensities in the high energy spectrum are remarkably high. The ^{28}Si intensity distribution from a silicon wafer as a function of secondary ion kinetic energy is plotted in Figure 2. The wafer potential was varied using an external power supply, while 4500 ± 10 eV ions were transmitted by the secondary column.

For nonconductor samples the specimen isolation method results in a SIMS spectrum in which the molecular ions are very strongly suppressed. This is illustrated in the spectrum of a zircon from McDonald Mine, Ontario, Canada (Figure 3). Molecular ion peaks where resolvable in this spectrum are almost exclusively due to monoxides of the major matrix elements. Element/oxide ratios decrease with increasing mass from 10^5 (for $\text{Si}^+ / \text{SiO}^+$) to 2×10^2 (for $\text{Th}^+ / \text{ThO}^+$).

Analysis of Minerals Using Specimen Isolated SIMS

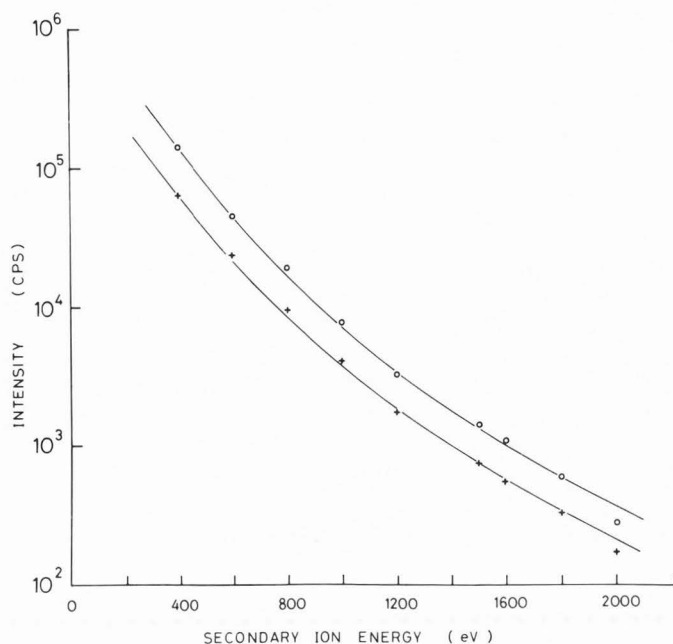


Figure 2. Intensity as a function of energy for $^{28}\text{Si}^+$ (o) and $^{29}\text{Si}^+$ (+) secondary ions, measured from a pure Si wafer coupled to an external power supply. Primary beam = 25 nA $^{16}\text{O}^-$, energy slits = 20 eV.

Interferences from multiply charged elemental ions are, in fact, more of a potential problem, with $1^+/2^+$ ratios over an order of magnitude lower in the high energy spectrum, and as low as 27 ± 5 (for $\text{Ca}^+/\text{Ca}^{2+}$). Fortunately, such interferences are usually distributed at half and integral M/e values. Thus they interfere with fewer peaks than molecular ions, and in most cases can be relatively easily corrected for.

The advantages in sensitivity of SIMS over X-ray based analytical methods are clear in the zircon spectrum (Figure 3), with close to forty elements positively identified. The spectral data was obtained in the space of five minutes. The resolution of the complete rare earth series is notable as the Rare Earth Elements distribution pattern is readily calculated⁹ directly from the intensity data. MacRae and Metson⁷ have measured Rare Earths at 100 ppb levels using this approach. These levels of the heavy Rare Earths have not been satisfactorily resolved with either conventional energy filtering or high mass resolution^{12,14}.

Elemental ion intensities from the zircon spectrum show reasonable agreement with natural isotopic abundances (Table 1). However one observes a clear fractionation towards lighter isotopes, consistent with previous SIMS observations of isotope effects^{3,15,17,18}, but considerably larger than those previously reported. Fractionation factors (F.F.) as large as 33% are apparent in Table 2, where:

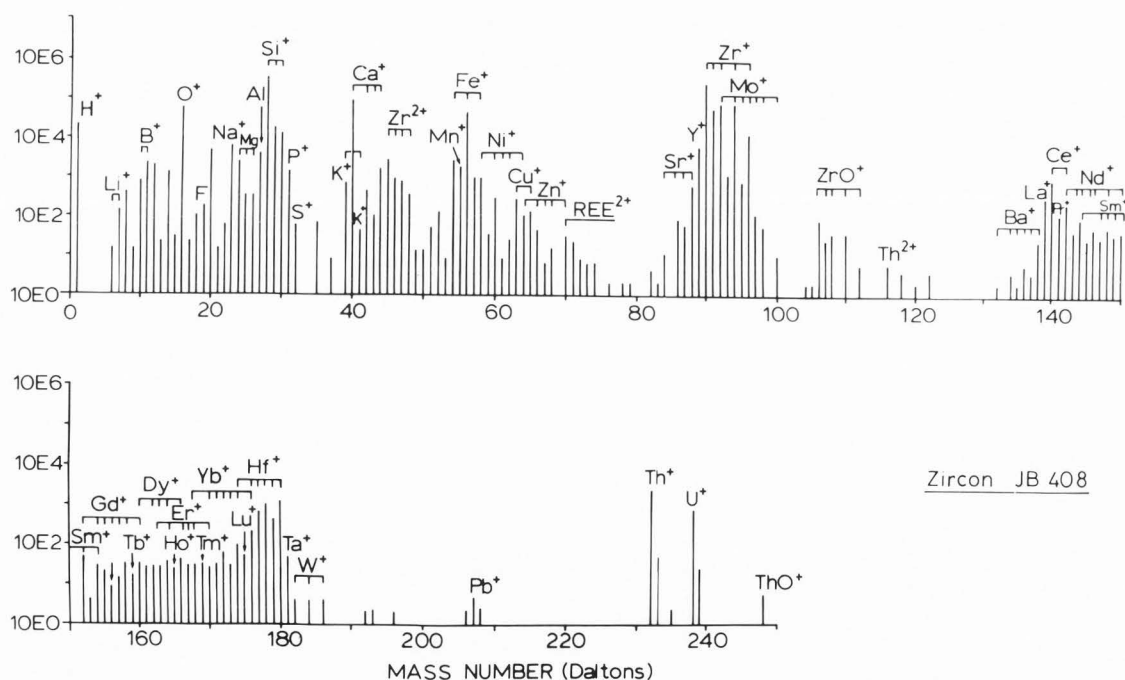


Figure 3. The secondary ion mass spectrum (bar graph) of a zircon crystal from McDonald Mine, Ontario, Canada. Count time = 1 sec/mass unit. Ion intensities reach constant values after 1 minute of sputtering. This spectrum was obtained before the primary beam mass filter was installed, thus the peaks attributed to Ni^+ are probably contaminants from the primary beam. The peaks at $M/e = 233$ and 239 do not represent hydrides but are due to the broad and noncentred 232 and 238 peaks respectively. Peaks at $M/e = 12, 13, 14$ and 15 are due to $^{12}\text{C}^+$, $^{13}\text{C}^+$, $^{28}\text{Si}^{++}$, and $^{30}\text{Si}^{++}$ respectively.

$$F.F. = \frac{(L/H)_{\text{observed}}}{[(L/H)_{\text{absolute}}^{-1}] \times 100} \quad (1)$$

L = intensity of lighter isotope, H = intensity of heavier isotope. We believe these large values result from the analysis of secondary ions of much higher kinetic energies than those observed in previous reports of this type of isotope effect (>500 eV compared to 0 - 80 eV). Isotope measurements in SIMS experiments have been and are still very difficult to make. However two features of the high energy secondary ion spectrum simplify measurements in this energy region. One of the major problems in isotope measurements is the instability of the secondary ion signal whether due simply to primary beam instability, the dynamic nature of the sputtering process or introduced by the method used to eliminate molecular ion interferences. High mass resolution, which is the preferred method of ensuring unequivocal peak identification, requires extremely high instrument stability particularly in the magnetic sector¹ and is restricted to elements where the relevant molecular ions can be resolved without prohibitive loss of intensity. In the SI mode, although molecular ions are by no means eliminated, they are strongly suppressed to a degree where isotope measurements are possible under far less rigorous instrumental conditions than if mass resolution in excess of ~ 4000 were required.

The second feature of isotopic measurements is that the observed instrumental mass fractionation is a function of secondary ion energy, and appears to increase with increasing energy. This neither helps nor hinders the resolution of geochemical isotopic anomalies, however the observed ratios must be accurately corrected on the basis of the energy of the analyzed ions.

In this series of measurements, isotope intensities were determined relative to the intensity of $^{28}\text{Si}^+$. Thus the errors reported include the reproducibility of the $^{28}\text{Si}^+$ intensity.

The first question which must be addressed is the reproducibility of isotope measurements. The simplest case is summarized in Table 3. A NBS standard Si wafer of known isotopic composition (990) was isolated from the sample holder with a Teflon spacer (see Figure 1) following the normal S.I. procedure. From a mass spectrum of the silicon isotopes, magnetic field parameters¹³ were obtained for $^{28}\text{Si}^+$, $^{29}\text{Si}^+$ and $^{30}\text{Si}^+$. Six determinations were then made of the Si isotope abundances with four measurements in each determination. Count times of 1, 2, 4, 4, 8 and 16 seconds per isotope were used in the six blocks. The results are shown in Table 3 together with a second set of measurements on the same wafer obtained several hours later after remounting the sample in a second sample holder, again with a 3mm aperture size and Teflon insulation. Surface charging was measured by scanning of the electrostatic analyzer to the position of peak secondary ion intensity², which was assumed to represent 0 ± 5 eV ions.

From Table 3 it is apparent that under these conditions (semiconducting sample, Teflon insulated, surface charge 430 ± 10 eV), isotope measurements for major elements can be made with considerable reproducibility. It is also

apparent that even analyzing such high energy species there is a measurable contribution of $^{28}\text{SiH}^+$ to $^{29}\text{Si}^+$. From the deviation of $^{28}\text{Si}^+ / ^{29}\text{Si}^+$ and $^{29}\text{Si}^+ / ^{30}\text{Si}^+$ from the theoretical (mass dependent) fractionation line, it is possible to estimate a ratio of $^{28}\text{Si} / ^{28}\text{SiH}^+ \sim 5 \times 10^4$. This is slightly lower than the ratios observed in bargraph spectra, $^{30}\text{Si} / ^{30}\text{SiH}^+ \sim 3 \times 10^5$.

Measurements on natural mineral samples are considerably more difficult, particularly if the fractionation of less abundant elements is of interest. Intra-measurement reproducibility is proportional to secondary ion intensity. In the zircon sample, standard deviations for $^{90}\text{Zr} / ^{92}\text{Zr}$ (z = 90, 91, 92, 94, 96) range from 0.1 to 0.4% over four measurements with four cycles within each measurement. This is irrespective of whether the peak positions are determined by (a) manual adjustment of the magnetic field (b) auto calibration by step scanning over the peak or (c) magnetic field parameters determined from the mass spectrum. The opposite extreme is represented by light trace elements where low intensities and narrow peaks make field adjustment and machine stability critical. Standard deviations for $^6\text{Li}^+ / ^{28}\text{Si}^+$ ranged from 3 to 7% over blocks of four cycles.

The measurement to measurement stability in determining isotope ratios is summarized in Table 2. In all cases except Li 6/7, σ lies between 0-3% (Zr) and 5% (B & Mg). In the case of Li, the ratios where the combined $^6\text{Li}^+ / ^{28}\text{Si}^+$ and $^7\text{Li}^+ / ^{28}\text{Si}^+$ errors were greater than 5% were rejected (both from the mass spectrum), leaving only two of the four determinations. It is clear from the relationship between σ and the observed intensity, that the ability to determine isotopic ratios is determined largely by counting statistics rather than any variation in the isotope ratios themselves due to effects such as differential charging which would influence all elements.

The fractionation factors we observed vary almost linearly with M_H / M_L (Figures 4(a) and 4(b)), indicating a purely mass related effect,¹⁵ in line with the observation of Shimizu and Hart.¹⁵ In terms of the formalism proposed by Slodzian et al.¹⁸, this means that in the 400-700 eV secondary energy region, within a given matrix, the parameter $\alpha = FF / \Delta M_{HL} / M_L$ is similar for all elements i.e. there is no resolvable element effect as is observed with low energy secondaries³. The value of α (equivalent to the slope of the FF vs M_H / M_L plot) is determined by the degree of surface charging.

The population of sputtered neutrals plus ions must, in equilibrium,¹⁵ reflect the composition of the bulk material. Thus mass related isotopic effects must predominantly be introduced in the process of ionization (assuming angular distribution effects are small) and selectivity is clearly enhanced in the higher energy secondary ion spectrum.

Secondary ions are assumed to be sputtered predominantly as neutrals and are subsequently ionized as they cross the surface energy barrier. Thus the enhanced degree of isotopic fractionation we observe is also a potential tool for the investigation of the ionization process. The assumption

Analysis of Minerals Using Specimen Isolated SIMS

TABLE 1

Observed isotopic ratios and fractionation factors in the Secondary Ion Mass Spectrum of McDonald Mine Zircon

Element	Isotope pair	Mass Spectrum		Isotope		Average ratio	Absolute ratio	Fractionation factor
		Integrated	Peak top	Peak	top			
Li	6:7	[0.083]	[0.065]	0.093	0.097	0.095±0.3	0.080	18.8 ± 5.0
B	10:11	0.265	0.257	0.278	0.253	0.26 ±0.01	0.244	7.8 ± 4.5
Mg	24:26	7.38	7.44	8.15	8.38	7.84 ±0.5	7.18	9.2 ± 6.9
Si	28:29	20.6	20.8	20.7	20.4	20.6 ±0.2	19.62	5.0 ± 1.0
	28:30	32.5	33.8	30.9	32.4	32.4 ±1.2	29.84	8.6 ± 4.0
Ca	40:42	154	152	162	166	159 ± 6	151.6	4.9 ± 4.5
Fe	54:56	0.0664	0.0668	0.0654	0.0670	0.0664±0.0008	0.0635	4.6 ± 1.3
Sr	86:88	0.123	0.130	0.116	0.130	0.125±0.007	0.119	4.8 ± 6.0
Zr	90:94	3.11	3.07	3.09	3.11	3.09±0.02	2.960	4.4 ± 1.4
	90:96	19.8	19.9	19.7	19.8	19.8±0.1	18.39	7.67±0.55
Hf	177:180	0.545	0.534	0.541	0.537	0.538±0.005	0.526	2.28±0.95

TABLE 2

Isotope ratios observed using the mass spectrum for a synthetic sphene (CaTiSiO₅) ceramic

Element	Isotope pair	Observed ratio	Absolute ratio	Fractionation factor
B	10:11	0.325	0.244	33.3
Mg ^a	24:26	9.01	7.182	25.4
Si	28:29	22.3	19.62	13.5
	28:30	37.0	29.84	24.0
Ca	29:30	16.6	15.21	9.3
	40:42	187.8	151.6	23.9
Ti ^b	40:44	62.8	47.10	33.4
	47:49	1.50	1.321	13.3
Sr	47:50	1.62	1.363	18.9
	48:50	15.9	13.84	14.9
Zr ^c	86:87	1.45	1.405	3.2
	86:88	0.123	0.1194	2.8
Mo	90:91	4.84	4.598	5.2
	95:100	1.87	1.630	14.8
	98:100	2.68	2.471	8.6

(a) ²⁴Mg⁺ has been corrected for interference from ⁴⁸Ti⁺⁺. This was done on the basis of the intensities of ⁴⁷Ti⁺⁺ and ⁴⁹Ti⁺⁺ at M/e = 23.5 and 24.5 respectively. The uncertainty in 24:26 is thus considerably greater (±7%) than the other elements considered.

(b) ⁴⁸Ti⁺ must be corrected for interference from ⁴⁸Ca⁺. This was done from the intensity of ⁴⁰Ca⁺ together with the predicted fractionation of ⁴⁸Ca⁺:⁴⁰Ca⁺.

(c) These two are the only Zr isotope ratios not affected by overlap with large Mo peaks, (⁹²Zr⁺, ⁹⁴Zr⁺ and ⁹⁶Zr⁺).

TABLE 3

Isotope ratios from pure silicon SRM990 under Specimen Isolated conditions

Isotope pair:	holder 1	holder 2	Absolute	Mean F.F. (%)
28/29	20.80±0.06	20.7±0.1	19.75	5.06±0.04
28/30	33.3 ±0.2	33.14± 0.2	29.74	11.63±0.14

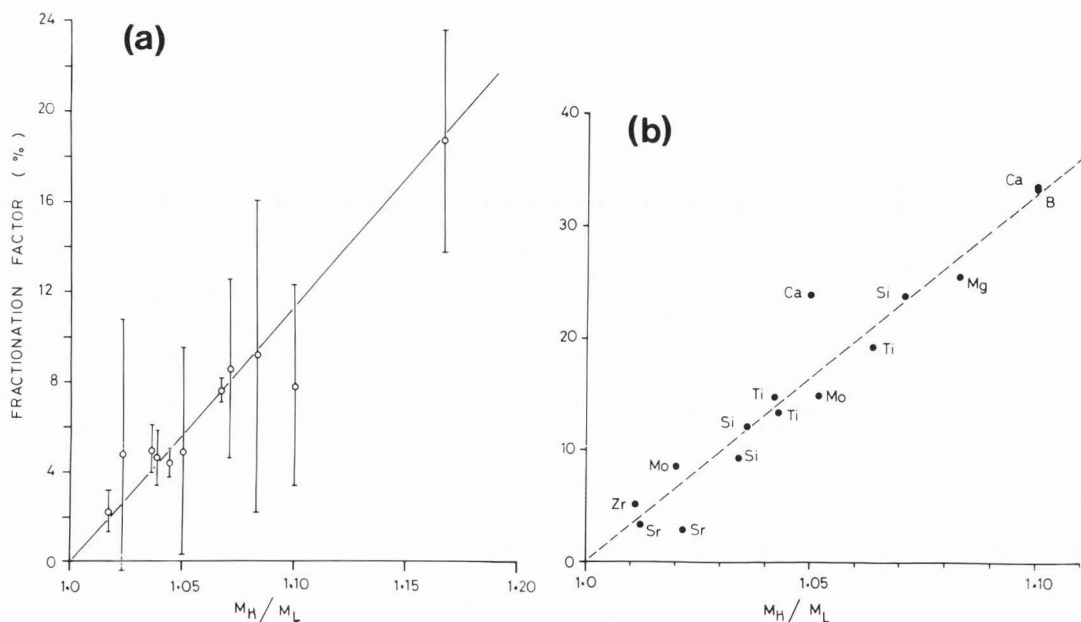


Figure 4. A plot of fractionation factor FF vs. mass ratio (M_H/M_L) for (a) the McDonald Zircon crystal and (b) a synthetic sphene ($CaTiSiO_5$). The data used are drawn from Tables 1 and 2. Because of duoplasmatron problems, we were limited to small primary beam current (~ 5 nA) in Figure 4a. This is reflected in lower surface charging and thus limited offset was achieved. For example, the hydride contributions at $M/e = 178$ and 179 make these peaks impossible to use. This is not a problem in the sphene spectrum run earlier (~ 90 nA primary current) and this is reflected in larger and more consistent FF values.

that angular distribution effects are small certainly needs further investigation in this range of secondary ion energies and surface charge distributions. Preliminary investigations of the role of the contrast aperture (controlling acceptance angle of secondary ion trajectories), suggest measurable effects and this is under further investigation.

High sensitivity for a wide variety of elements can also be of considerable use in in-situ examination of small phases within minerals and mineral assemblages. The ability to scan across a surface gives the capability for three dimensional analysis of a mineral surface. A line scan of a sphene [$CaTiSiO_5$], hornblende [$(Na,K)_{0-1}Ca_2(Mg,Fe,Al)_5Si_8O_{22}(OH)_2$] contact is shown in Figure 5, illustrating the capability to follow both major and trace elements across a large and complex alteration zone between the minerals. Comparison of the chemical compositions of the two minerals (from the electron microprobe) and SIMS intensities shows that matrix effects are relatively unimportant - at least for these high energy ions. Thus, in qualitative agreement with the SIMS data, the electron probe analyses (Table 4) show that the Si analyses (30% SiO_2 for the sphene and 52% for the hornblende) change by only

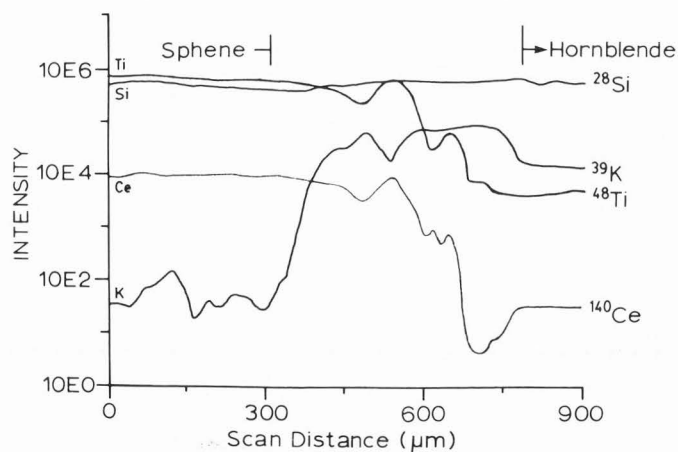


Figure 5. Line scans of four elements across a sphene/hornblende contact. This sample is from Bear Lake Rd., Ontario, Canada and is the junction of a large sphene crystal and a surrounding hornblende matrix.

Analysis of Minerals Using Specimen Isolated SIMS

TABLE 4

Electron Probe Analyses of Bear Lake Sphene and Hornblende ~1.0 mm from contact

	<u>Sphene</u>	<u>Hornblende</u>
SiO ₂	30.32	53.25
CaO	27.35	7.90
TiO ₂	37.54	0.1
MgO	0.01	17.67
Al ₂ O ₃	0.38	1.13
FeO	1.46	9.64
K ₂ O	-	1.33
Na ₂ O	0.36	4.92
MnO	0.05	0.36
Nb ₂ O ₅	1.00 <u>98.48</u>	- <u>96.24</u>

a factor of 1.7; the Ce levels in the hornblende (~20-40 ppm) are two orders of magnitude lower than in the sphene (~1600 ppm determined by neutron activation), and the Ti level in the sphene (37.5% TiO₂) is two orders of magnitude larger than in the hornblende (<0.1). It is interesting that the K⁺ and Ce⁺ profiles which should mark the interface between the two minerals, do not appear to correspond: the rise of K⁺ and decline in Ce⁺ are separated by ~300 μm.

The high levels of elemental/molecular ion discrimination observed improve prospects for quantitative analysis for many elements in silicates (Nesbitt et al¹¹ - 1985). One example of this is phosphorus determination in silicates. The resolution of ³¹P⁺ from ³⁰Si¹H⁺ has been a major use of the high mass resolution capabilities of magnetic sector based SIMS instruments. Using the specimen isolated method we have analyzed a series of whole rock powders with known phosphorus concentrations. Specimens were prepared as fused discs in a Pb₂SiO₄ glass matrix. This presents an extreme example of the P determination problem, as silicon is the dominant matrix element. Under specimen isolated conditions, measured ³¹P⁺/²⁸Si⁺ values when plotted against the rock powder P levels form a straight line passing (within experimental error) through the origin (Figure 6). Thus the ²⁰Si¹H⁺/³⁰Si⁺ intensity ratio is less than 3X10⁻⁴ in these silicate matrices, making it possible to determine phosphorus levels to below 0.01% P₂O₅ with no corrections for interference, provided suitable standards are available. Although in this case the phosphorus peak can be readily resolved using moderate mass resolution (M/ΔM~4000), the same is not true, for example, for resolving the heavy rare earth elements, from the light rare earth oxides¹². MacRae & Metson⁷ have measured ¹⁵⁵(LaO)⁺/¹³⁹La⁺ ratios <10⁻³ under specimen isolated conditions.

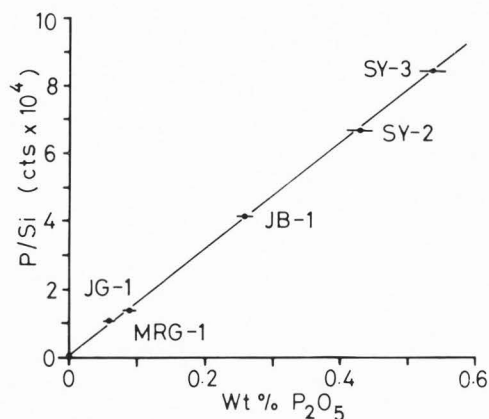


Figure 6. A plot of ³¹P⁺/²⁸Si⁺ intensities versus phosphorus concentration for a series of analyzed rock powders incorporated in lead silicate glasses. Error bars represent 10% variations in the rock standard P values. Standard deviations in the SIMS measurements ranged from 2.3% (SY-2) to 5.4% (JG-1) over 4 cycles of 2 seconds. Thus the counting errors are small relative to the horizontal error bars.

Conclusions

It is clear that SIMS has considerable potential in geochemical analysis as an eventual substitute for a number of analytical methods currently employed. The use of specimen isolation provides greater suppression of molecular ions than has been reported in the conventional application of energy filtering and has considerably broader application than high mass resolution. The major drawback in utilizing this method is the current restriction on analysis area (~50 μm), which limits the analysis of small phases.

As well as simplifying the interpretation of spectra, the side effects of analyzing a relatively high energy secondary ion population are potentially interesting in their own right. The increased yield of multiply charged ions and the relationship of secondary ion energy to isotopic fractionation provide tools for the investigation of the fundamentals of the ionization process.

There is also the prospect that higher energy ions, as we analyze with this method, will be less susceptible to some of the matrix effects which influence the main low energy secondary ion population. Further experiments are being undertaken to investigate this possibility.

Acknowledgements

We would like to thank Dr. N. Shimizu for the loan of SRM 990. The helpful comments of Dr. N.S. McIntyre are acknowledged, along with the assistance of W.J. Chauvin and D. Johnston for technical expertise, and the Natural Sciences & Engineering Research Council and the University of Western Ontario for financial assistance.

References

1. Huneke, J.C., Armstrong, J.T., Wasserburg, G.J. (1983) FUN with PANURGE: High mass resolution ion microprobe measurements of Mg in Allende inclusions. *Geochim. Cosmochim. Acta*, **47**, 1635-1650.
2. Lau, W.M., McIntyre, N.S., Metson, J.B., Cochrane, D., Brown, J.D. (1985) Stabilization of charge on electrically insulating surfaces - experimental and theoretical studies of the specimen isolation method. *Surface and Interface Analysis* (in press).
3. Lorin, J.C., Havette, A., Slodzian, G. (1982) Isotope Effect in Secondary Ion Emission. *SIMS III*, 140-149, Springer Verlag, Berlin.
4. Lovering, J.F. (1975) Applications of SIMS microanalysis techniques to trace element and isotopic studies in Geochemistry and Cosmochemistry. *NBS Spec. Publ.*, Washington, DC 20234, **427**, 135-178.
5. McIntyre, N.S., Chauvin, W.J., Metson, J.B., Bancroft, G.M. (1984) Suppression of Molecular Ions in Secondary Ion Mass Spectra, *J. de Physique, Colloque C2*, **45**, 143-146.
6. McIntyre, N.S., Fichter, D., Robinson, W.B., Metson, J.B., Chauvin, W.J., (1985) Suppression of Molecular Ions in SIMS Spectra of Metals and Semiconductors. *Surface and Interface Analysis* **7** (2), 69-73.
7. MacRae N.D., Metson, J.B. (1985) In-situ rare earth element analysis of coexisting pyroxene and plagioclase by secondary ion mass spectrometry. *Chemical Geology*, in press.
8. Metson, J.B., Bancroft, G.M., McIntyre, N.S., Chauvin, W.J. (1983) Suppression of Molecular Ions in the Secondary Ion Mass Spectra of Minerals. *Surface and Interface Analysis* **5** (5), 181-185.
9. Metson, J.B., Bancroft, G.M., Nesbitt, H.W. and Jonasson, R.G. (1984) Analysis for Rare Earth Elements in accessory minerals by Specimen Isolated Secondary Ion Mass Spectrometry. *Nature* **307**, 347-349.
10. Metson, J.B., Bancroft, G.M., McIntyre, N.S., Chauvin, W.J. (1984) Molecular Ion Suppression in the Secondary Ion Mass Spectra of Minerals. *SIMS IV*, 466-468, Springer Verlag, Berlin.
11. Nesbitt, H.W., Metson, J.B., Bancroft, G.M. (1985) Quantitative major and trace element whole rock analysis by Secondary Ion Mass Spectrometry. (Internal Report, copy available from J.B. Metson)
12. Reed, S.J.B. (1981) Secondary Ion Spectra of Rare Earths - in *Microbeam Analysis - 1981*. R.H. Geiss (ed), San Francisco Press, San Francisco, 87-90.
13. Robinson, W.H., Johnston, D. (1984) Manual for the Cameca IMS-3f software. Report SSW-014 (available from Surface Science Western, University of Western Ontario).
14. Shimizu, N., Hart, S.R. (1982) Applications of the ion microprobe to Geochemistry and Cosmochemistry. *Ann. Rev. Earth Planet. Sci.* **10**, 483-526.
15. Shimizu, N., Hart, S.R. (1982) Isotope fractionation in secondary ion mass spectrometry. *J. Appl. Phys.* **53**(3), 1303-1311.
16. Shimizu, N., Semet, M.P., Allegre, C.J. (1978) Geochemical applications of quantitative ion microprobe analysis. *Geochim. Cosmochim. Acta* **42**, 1321-1334.
17. Slodzian, G. (1982) Dependence of Ionization yields upon Elemental Compositions; Isotopic variations. *SIMS III*, 115-123. Springer Verlag, Berlin.
18. Slodzian, G., Lorin, J.C., Havette, A. (1980) Isotope effect on the Ionization Probabilities in Secondary Ion Emission. *J. de Phys. Lett.* **41**, 555-588.
19. Werner, H.W., Morgan, A.E. (1976) Charging of insulators by ion bombardment and its minimization for secondary ion mass spectrometry (SIMS) measurements. *J. Appl. Phys.* **47** (4), 1232-1242.

Discussion with Reviewers

P. Williams: Given the accepted fact that intensities fall monotonically with energy from the low energy maximum, how can S.I. filtering give better intensity than conventional filtering with the same energy window?

Authors: We cannot satisfactorily account for the magnitude of the intensities seen under S.I. conditions. However we have identified several contributing factors which favour energy filtering at the sample surface by this method. The first is that the energy window is not the same. With increasing secondary ion energy the contrast aperture appears to control the width of the energy window. At 500 eV with a fully open contrast aperture the effect is substantial and is accompanied by a decrease in the apparent mass resolution. A second factor is the large primary beam currents limited in our case only by what the duoplasmatron will deliver (100 → 200 nA), which can be stabilized on insulator surfaces under these conditions (with correspondingly large beam diameters).

P. Williams: Given that differential charging across the surface of an insulating sample garbles the ion image, what are the prospects for microanalysis with this technique?

Authors: The "garbling" of images from a charging surface results from the effects of a non-uniform electric field above the surface bending ion trajectories. However this effect is most pronounced for low energy (0 → 50 eV) secondaries

which are readily bent. Images from higher energy secondaries are less distorted. Thus, even from the Cu/Al grid under S.I. conditions it is necessary to image ions of energies close to or greater than the surface charge. Thus 0→300 eV ions yield no image detail, while 500→600 eV ions are relatively undistorted except for a beam directed near the edge of the sample holder. The field lines above such a surface are discussed in reference 2. In the case of an insulating sample, the critical consideration is how "differential" the charging is. It is extremely difficult to measure charge distribution across such a surface, however computer simulation studies indicate that with a large beam and a $1/r^2$ charge distribution, the trajectories of 500 eV secondaries (as are typically obtained under these conditions) are not significantly distorted and should be "imagable".

An interesting alternative approach is to gold coat the surface anyway and insulate it below the same aperture. Charge distribution problems are somewhat simplified under these conditions while the secondaries analyzed are still 450→550 eV.

Microanalysis probably still hinges on achieving the same degree of charging with smaller beams and thus smaller currents. A corresponding reduction in aperture size is required and the effect of this on sensitivity and stability has not yet been examined.

S.J.B. Reed: No allowance is made for ion yield variations between the rare earth elements, which have been found to vary by a factor of at least 5 (ref. 12). Has any investigation of REE yields under S.I. conditions been made, as is necessary to quantify results?

Authors: Rare earth element ion yields have been investigated and are discussed in reference 7. They do not differ significantly from those in reference 12 apart from a compression in range between the most and least sensitive.

S.J.B. Reed: Is it known approximately what the effective energy threshold is in this form of secondary ion filtering, also what fraction of the secondary ions are utilized?

Authors: The effective energy threshold can be and has now been measured quite accurately on a wide range of samples. All the samples analyzed both insulators and conductors, fall in the 450→700 eV range with most distributed around 500 eV (3 mm aperture 100 nA 160°). As far as fraction of secondaries utilized, that depends on the energy distribution of the species being investigated. It is probably highest for the rare earths and heavier elements at ~1→3% and at least an order of magnitude lower for Al, Si etc.

